ORIGINAL ARTICLE

Veterinary Research Forum. 2024; 15 (4): 171 - 179
doi: 10.30466/vrf.2024.2011271.4007
Journal Homepage: vrf.iranjournals.ir

Veterinary Research Forum

Key molecules regulating the blood meals of *Rhipicephalus sanguineus* (Acari: *Ixodidae*) revealed by transcriptomics

Yajun Lu[1,2,3], Yijia Xu[3], Chenghang Yu[1], Shi Cheng[3], Qianfeng Xia[3]*, Zheng Bin[1]*

[1] National Institute of Parasitic Diseases, Chinese Center for Disease Control and Prevention (Chinese Center for Tropical Diseases Research), NHC Key Laboratory of Parasite and Vector Biology, WHO Collaborating Center for Tropical Diseases, National Center for International Research on Tropical Diseases, Shanghai, China; [2] Department of Pathogen Biology and Immunology, School of Basic Medical Sciences, Xi'an Jiaotong University, Xi'an, China; [3] Key Laboratory of Tropical Translational Medicine of Ministry of Education, NHC Key Laboratory of Tropical Disease Control, School of Tropical Medicine, Hainan Medical University, Haikou, China.

Article Info

Article history:

Received: 18 September 2023
Accepted: 08 January 2024
Available online: 15 April 2024

Keywords:

Blood meal
Hematophagy
Rhipicephalus sanguineus
Tick-host interactions
Transcriptomics

Abstract

Rhipicephalus sanguineus, a repulsive obligate blood feeder, is a three-host tick inflicting tremendous damage. Blood-sucking initiates tick-pathogen-host interactions along with alterations in the expression levels of numerous bioactive ingredients. Key molecules regulating blood meals were identified using the transcriptomic approach. A total number of 744 transcripts showed statistically significantly differential expression including 309 significantly upregulated transcripts and 435 significantly downregulated transcripts in semiengorged female ticks compared to unfed ticks, all collected in 2021. The top 10 differentially upregulated transcripts with explicit functional annotations included turripeptide OL55-like protein, valine tRNA ligase-like protein and ice-structuring glycoprotein-like protein. The top 10 differentially down-regulated transcripts were uncharacterized proteins. Gene Ontology (GO) enrichment analysis revealed four associated terms in the cellular component category and 16 in the molecular function category among the top 20 terms. Differentially expressed genes (DEGs) were enriched in GO terms ID 0000323 (lytic vacuole) and ID 0005773 (vacuole). The top 20 enriched Kyoto Encyclopedia of Genes and Genomes (KEGG) pathways included metabolism, cellular processes, organismal systems and human diseases. The DEGs were enriched in the KEGG term ID: ko-04142 (lysosome pathway) associated with intracellular digestion in the tick midgut epithelium. Molecular markers annotated via comparative transcriptomic profiling were expected to be candidate markers for the purpose of tick control.

Introduction

Rhipicephalus sanguineus (Acari: *Ixodidae*), also known as the brown dog tick, is an obligate bloodsucking ecto-parasite with a cosmopolitan distribution.[1] In recent years, a noticeable increasing trend in the prevalence of tick-borne infectious diseases has been emphasized and attributed to a wide range of pathogens transmitted by ticks with a high vectorial capacity.[2,3] The *R. sanguineus,* the prominent vector for transmitting *Babesia vogeli*, *Ehrlichia canis*, and *Rickettsia conorii,* affect animal health and cause economic losses.[4-7] The larva, nymph and adult of the three-host tick *R. sanguineus* all engorge primarily on dogs, occasionally attach to humans and feed on different hosts for each life stage.[8,9] Also, *R. sanguineus* transmits query fever,[10] Mediterranean spotted fever,[11] rocky mountain spotted fever[12] and bartonellosis[13] that seriously jeopardize human health resulting in illness, disability and death.

Blood meals initiate tick-pathogen-host interactions and induce a range of changes in the internal anatomy of ticks.[14,15] The tick salivary gland (SG), located at the anterior end, is the first gateway for blood-feeding and essential for successfully obtaining a blood meal at the tick-host interface. The start of the blood meal is accompanied by increases in tick size, weight and protein

***Correspondences:**

Qianfeng Xia. PhD
Key Laboratory of Tropical Translational Medicine of Ministry of Education, NHC Key Laboratory of Tropical Disease Control, School of Tropical Medicine, Hainan Medical University, Haikou, China
E-mail: xiaqianfeng@hainmc.edu.cn
Zheng Bin. PhD
National Institute of Parasitic Diseases, Chinese Center for Disease Control and Prevention, Chinese Center for Tropical Diseases Research, Key Laboratory of Parasite and Vector Biology, National Health Commission, WHO Centre for Tropical Diseases, National Center for International Research on Tropical Diseases, Ministry of Science and Technology, Shanghai, China
E-mail: zhengbin@nipd.chinacdc.cn

content. The salivary fluid is secreted in increased quantities with gradual acceleration during the feeding process.[16,17] As ticks complete a blood meal to achieve engorgement a few days later, the dilated SGs degenerate in response to physiological process transition. Saliva provides a rich supply of bioactive ingredients with anti-hemostatic, anti-inflammatory and immunomodulatory effects to obtain a continuous blood meal.[18]

The tick midgut (MG) is the largest organ in adult ticks and a major tissue involved in blood feeding. Storage of blood from the mammalian host, blood meal digestion and blood nutrient absorption proceed in MG under the impetus of diverse proteins secreted by the MG. During a prolonged period of sucking, a large amount of blood in the MG flows in a fluid state instead of coagulating. Blood digestion with great slowness in the epithelial cells of MG undergos dramatic alterations following blood acquisition.[19] Unlike other hematophagous insects, such as mosquitoes that absorb a blood meal in a rapid manner within the MG lumen, ticks consume blood in an intracellular mode.[20]

The tick ovary (OV) is the organ responsible for reproduction and closely related to the blood meal supply. An unfed female tick has small OVs and undeveloped oocytes. Acquisition of exogenous blood stimulates the OVs to dilate and the oocytes to begin accumulating nutritional components followed by further development and progressive maturation of the oocytes. Engorgement is essential for the development of ovarian tissue in female ticks especially the exogenous availability of heme in vertebrate blood which promotes embryogenesis.[21,22]

Tick hemolymph, characterized by an abundance of proteins and in which the internal organs are immersed, is the center of metabolic responses and the medium of substance exchange.[23] The ingestion of blood meals produces large changes in transcript levels and protein content in the hemolymph which also supports the migration of pathogens from vertebrate blood and the upregulation of molecules involved in tick innate immunity and molecules with anticoagulant effects.

Regarding notorious blood-feeders, exploration and research have been advancing and never stopped.[24] This study characterizes the differentially expressed transcripts in unfed and semiengorged female ticks via comparative transcriptomic profiling to identify key molecules involved in blood meals to elaborate the details in tick-host interaction network. Ticks bite and attach to the external surface of human and animal hosts skin, and subsequently remain to feed on the hosts until complete engorgement successfully. The blood feeding events generate lesions to the hosts via inhibiting the hemostasis, immunity and inflammation of hosts.[25] Key molecules involved in tick-host interaction network, which likewise interfere with the interactions through artificial repression or overexpression, are potential candidates for developing novel insecticides to block tick-host interactions.

Materials and Methods

Tick collection. Semiengorged female adult ticks of *R. sanguineus* were collected from the skin surface of stray dogs and unfed females were collected from dog kennels in March 2021. The semiengorged ticks and unfed ticks were placed into T25 cell culture flasks (25.00 cm^2 cell culture area) with a ventilation cap and brought back to the laboratory alive, after which they were surface cleaned with sterile phosphate-buffered saline solution.

RNA extraction, library construction and Illumina sequencing. Ticks in different feeding states were assigned to two groups of semiengorged ticks and 4 unfed ticks with three independent biological repetitions for each set. After the ticks were pulverized in a high-throughput tissue grinder (Scientz Biotechnology Company, Ningbo, China), total RNA was extracted using an EZ-10 Total RNA Mini-Prep Kit (BBI Life Sciences Corp., Shanghai, China) according to the manufacturer's protocol. The RNA quality was determined on an Agilent 2100 Bioanalyzer (Agilent Technologies, Palo Alto, USA) and screened by RNase-free agarose gel electrophoresis. Oligo (dT) beads were used to enrich eukaryotic mRNA in total RNA, while a Ribo-Zero™ Magnetic Kit (Epicentre Biotechnologies, Madison, USA) was used to remove ribosomal RNA (rRNA) and enrich prokaryotic mRNA. In fragmentation buffer, the enriched mRNA was fragmented into short fragments and reverse-transcribed into first-strand cDNA with NEBNext Random Primers employing NEBNext Ultra RNA Library Prep Kit for Illumina (New England Biolabs, Beverly, USA) according to instruction manual. Second-strand cDNA was synthesized by DNA polymerase I, RNase H and dNTPs, and the double-stranded cDNA fragments were purified using a QIAquick polymerase chain reaction (PCR) extraction kit (Qiagen, Venlo, Netherlands), end renovated, poly (A) appended and ligated to adapters for Illumina sequencing. The ligation products were size selected by agarose gel electrophoresis, PCR amplified and sequenced on the Illumina HiSeq2500 platform by Gene Denovo Biotechnology Company (Guangzhou, China).

***De novo* assembly and bioinformatics processing.** The RNA transcriptome raw data were generated using the Illumina sequencing platform and deposited in the Sequence Read Archive (SRA) database of the National Center for Biotechnology Information (NCBI). Raw reads including adapters or low-quality bases that could affect the subsequent assembly and analysis were further filtered by fastp Software (version 0.18; HaploX Biotechnology, Shenzhen, China) to exclude reads containing adapters, more than 10.00% unknown nucleotides or more than 50.00% low-quality bases (Q-value ≤ 20.00) and obtain high-quality clean reads.[26] The short read alignment tool Bowtie 2 Software (version 2.2; Johns Hopkins University, Baltimore, USA) was applied to map

reads to the rRNA database.[27] After removal of the mapped rRNA reads, the remaining clean reads were further employed for assembly and gene abundance calculation. An index of the reference genome was built and paired-end clean reads were mapped to the reference genome using HISAT2 Software (version 2.0; Johns Hopkins University) with "-rna-strandness RF" and other parameters set as the default.[28] The mapped reads of each sample were assembled using StringTie Software (version 1.3; Johns Hopkins University) in a reference-based approach.[29] For each transcription region, a fragment per kilobase of transcript per million mapped reads (FPKM) value was calculated to quantify expression abundance and variations using StringTie Software. The RNA differential expression analysis was performed by DESeq2 Software (version 1.20; Harvard School of Public Health, Boston, USA) between the two different groups,[30] the semiengorged tick group and unfed tick group to cluster differentially expressed genes (DEGs) and uncover differential transcript expression. Transcripts with a false discovery rate (FDR) < 0.05 and an absolute $\log_2$-fold change ($\log_2$FC) > 1 were considered as significantly differentially expressed transcripts. Correlation analysis was performed by R. Correlations between the two parallel experiments were tested to evaluate the reliability of the experimental results as well as the stability of the experimental operations. The correlation coefficient between two replicates was calculated to evaluate repeatability among samples. The closer the correlation coefficient was to 1, the better was the repeatability between two parallel experiments. Principal component analysis was performed with the R package gmodels (http://www.r-project.org) to reveal the relationship of the samples. All Gene Ontology (GO) terms were significantly enriched among DEGs compared to the genome background and the DEGs corresponding to biological functions were filtered by GO enrichment analysis. The DEGs were mapped to GO terms in the GO database (http://www.geneontology.org), gene numbers were calculated for every term and significantly enriched GO terms for the DEGs were defined by a hypergeometric test. The *p* values were adjusted by the FDR considering FDR-adjusted *p* value less than 0.05 significant. Kyoto Encyclopedia of Genes and Genomes (KEGG) pathway enrichment analysis was conducted on significantly enriched signal transduction pathways annotated in the KEGG database for DEGs compared to the whole genome background with the same calculation method used for GO analysis. FDR correction was applied to generate *p* values with FDR ≤ 0.05 as a threshold. Pathways meeting these criteria were interpreted as significantly enriched.

Functional annotation. Intake of blood is an essential physiological process for ticks and activates increases in transcript expression when a portion of genes are transcribed into mRNA and are positively regulated to promote expression, referred to as upregulated transcripts. In contrast, a portion of genes are negatively regulated during transcription into mRNA after blood intake by ticks which inhibits and decreases transcript expression levels, referred to as downregulated transcripts. Differentially expressed upregulated and downregulated transcripts were determined by a statistical significance test employing an FDR-adjusted *p* value < 0.05 and an absolute $\log_2$FC of > 1.00 as criteria for significance.

Results

Transcriptome data quality control analysis. The raw sequencing data from the transcriptomics were deposited in the NCBI SRA database under the BioProject accession number PRJNA983558, with SRA accession numbers SRR24966863 to SRR24966868 and BioSample accession number SAMN07728445. The semiengorged ticks were dispensed in three replicates encompassing groups S1, S2 and S3, and the unfed ticks were dispensed in three replicates encompassing groups U1, U2 and U3. To ensure data quality, data filtration was performed on raw data before information analysis to reduce any effects of invalid data on the analysis. The raw reads were quality controlled using fastp to exclude low-quality data and obtain clean reads, referred to as high-quality reads. The clean reads for the three groups of semiengorged ticks and the three groups of unfed ticks were obtained by removing adapter sequences and low-quality reads during raw read filtering, with the percentage of reads retained ranging from 99.71 to 99.74%. The base composition and quality distribution were analyzed to visualize data quality after data filtering. The more balanced the base composition, the higher the quality, leading to a more accurate subsequent analysis.

Sequence analysis. The distribution of the mapped reads that were *de novo* assembled was plotted on the reference genome and then divided into exons, introns and intergenic regions. More than 80.94% of the reads were distributed in exon regions with fewer (7.88 to 10.97%) in introns and (7.80 to 9.14%) intergenic regions. The transcriptomic data provided transcript expression information for a specific stage. The genes not annotated in the original reference genome were roughly identified by reassembling and recompiling the data. After transcriptome reconstruction, genes recognized in this sequencing step but not included in the reference genome were defined as novel genes. A total number of 3,477 clusters of unique transcripts devoid of any superimposed annotated genes were defined as novel genes. These novel genes plus the 23,522 genes in the reference genome combined to form a total number of 26,999 genes. The refined transcript reconstruction strongly supported the accuracy of the gene expression data. The FPKM value for each gene revealed the expression of transcripts in different groups

and was used to create a distribution map of gene expression for an assessment of the differences in library construction, sequencing and quantification among samples (Figs. 1A and 1B). A high FPKM value, log_{10}-transformed, indicated high gene expression.

Differential transcript expression analysis. A total number of 744 significantly differentially expressed transcripts were identified including 309 upregulated transcripts expressed at high levels and 435 downregulated transcripts expressed at low levels in the semiengorged ticks compared to the unfed ticks which also implied that a series of important physiological processes occurred during blood meals in the tick life cycle. A volcano plot was generated to display significantly differentially expressed transcripts and a heatmap was developed to present the hierarchical clusters of differentially expressed transcripts with similar expression patterns, sharing common functions or involved in common metabolic and signaling pathways (Figs. 1C and 1D). Out of the 309 upregulated transcripts, 77 novel and as yet unannotated genes were identified whereas out of the 435 downregulated transcripts, 95 novel and not yet annotated genes were identified. The IDs prefixed with MSTRG (MSTRG.ID) indicated that the identified gene was a novel gene. The 10 most upregulated genes including MSTRG.15337, MSTRG.20016, NCBI Gene ID (GI) 119373294, MSTRG.7358, MSTRG.5877, GI 119393210, MSTRG.20627, MSTRG.15121, GI 119399007 and GI 119396222 were listed in descending order. The four annotated upregulated genes including GI 119373294, GI 119393210, GI 119399007 and GI 119396222 were encoded different proteins. The annotated GI 119373294 gene encodes a turripeptide OL55-like protein distinguished as a cysteine-rich protein. The GI 119393210 gene encodes a protein for the valine tRNA ligase-like protein. The GI 119399007 gene encodes the ice-structuring glycoprotein-like protein recognized as the nucleic acid-binding protein from the mobile element jockey. The GI 119396222 gene is an uncharacterized protein-coding gene described as encoding the predicted timeless-interacting protein isoform X2. The 10 most downregulated genes were MSTRG.20238, MSTRG.19838, MSTRG.18613, MSTRG.18646, MSTRG.22972, GI 119383828, MSTRG.18623, MSTRG.15050, MSTRG.27111 and GI 119402726. Both of the annotated downregulated genes, GI 119383828 and GI 119402726, were uncharacterized protein-coding genes.

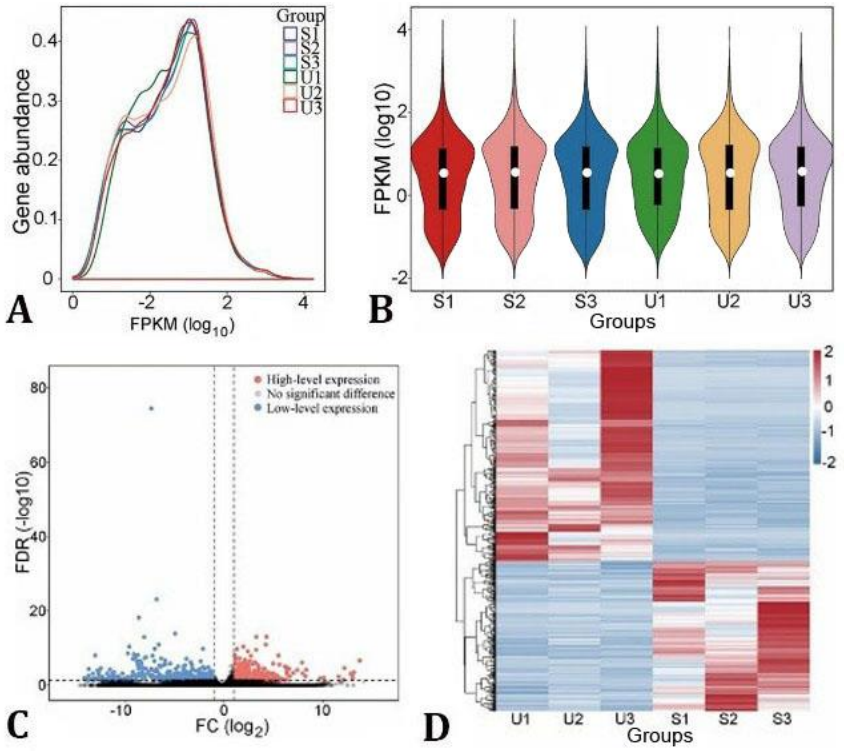

Fig. 1. Gene expression map and plot of differentially expressed transcripts. **A)** The X-axis represents log_{10} FPKM values and the Y-axis represents gene abundance, defined as the ratio of the number of genes corresponding to the X-axis value to the total number of expressed genes. The distribution curve shows a peak centered on the highest concentration of gene expression. **B)** Violin plot showing the changes in gene abundance. **C)** Volcano plot showing significantly differentially expressed transcripts with the blue dots indicating low-level expression, the red dots indicating high-level expression and the gray dots indicating no significant differential expression. Dots located closer to the two ends of the plot indicate greater differences in differentially expressed transcripts. **D)** Each column represents a group and each row represents a transcript in the hierarchical clustering heatmap. Different colors depict the transcript expression levels in different groups with redder colors indicating higher expression and bluer colors indicating lower expression.

Enrichment analysis. The GO analysis is a standardized procedure for gene function classification and describing genes and transcripts comprising three ontologies, namely, molecular function, cellular component and biological process. In the GO functional significance enrichment analysis the significant enrichment clusters of the differentially expressed transcripts were isolated as GO terms to predict biological functions. Out of the top 20 GO terms ranked by FDR-adjusted *p* values from smallest to largest, 4 were classified as cellular components and 16 were identified as molecular functions in the GO enrichment map (Figs. 2 and 3). The GO enrichment yielded two GO terms (GO IDs: 0000323 and 0005773) mapped by the DEGs that were associated with cellular components including 14 DEGs and 16 DEGs, respectively. However, no significant GO terms involved in molecular functions or biological processes were identified. The GO term ID 0000323 (lytic vacuole) was associated with the 14 DEGs with GI IDs 119372541, 119378357, 119378839, 119381061, 119386015, 119386803, 119389752, 119390930, 119390934, 119391070, 119396876, 119399694, 119402466 and 119405483. The GO term ID 0005773 (vacuole) was associated with the 16 DEGs with GI IDs 119372541, 119378357, 119378839, 119381061, 119384031, 119386015, 119386803, 119389752, 119390930, 119390934, 119391070, 119394421, 119396876, 119399694, 119402466 and 119405483. The two GO terms shared 14 DEGs.

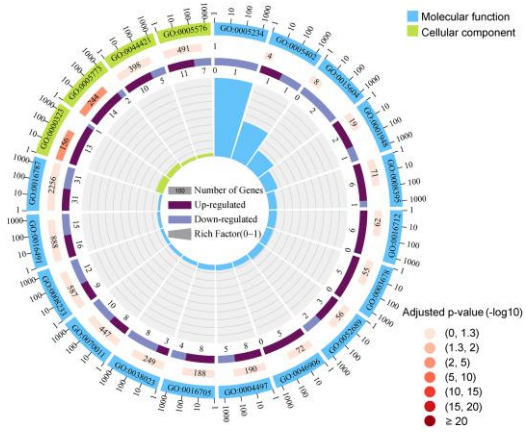

Fig. 2. Gene Ontology (GO) enrichment plot showed the top 20 GO items sorted by false discovery rate -adjusted *p* value from smallest to largest. The outside of the outermost circle is a co-ordinate scale for the number of DEGs, and the different colors of the outermost circle represent different ontologies with four items classified as cellular component ontology (green bars) and 16 items identified as molecular function ontology (blue bars). A longer bar represents a greater number of DEGs and a redder bar represents a smaller adjusted *p*-value in the second circle from the outside to the inside. The ratios of DEGs is demonstrated in the third of circle from the outside to the inside with dark purple representing the ratios of the up-regulated genes, light purple denoting the ratios of the down-regulated genes and the corresponding ratios displayed below. For each GO term, the innermost circle displays the rich factor values denoting the number of DEGs divided by the number of all genes with each grid in the light gray grid line representing 0.1.

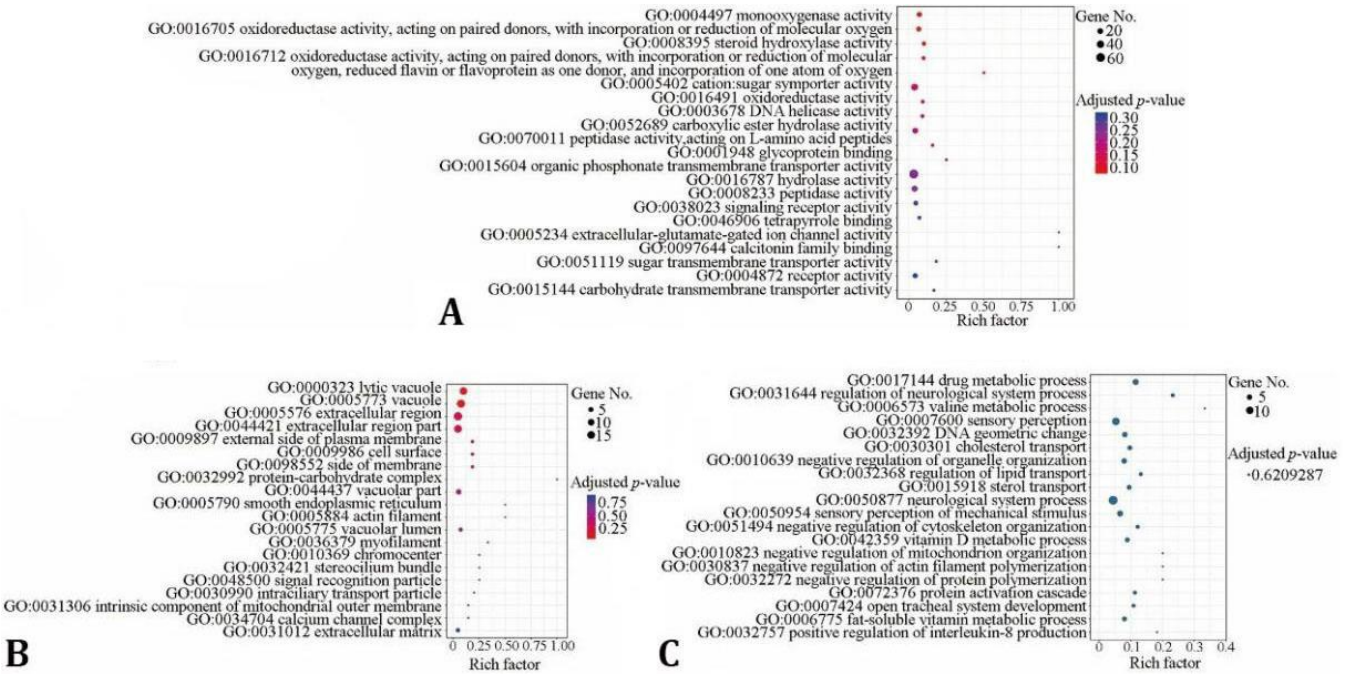

Fig. 3. A, B and **C)** The GO enrichment bubble plot where bubble size indicates the number of genes and a redder bubble denotes a smaller adjusted *p* value. The Y-axis shows the categories, namely, molecular function, cellular component and biological process and the X-axis shows the enrichment factor.

The KEGG pathway enrichment analysis helps elucidate the biological functions of genes and provides statistically significant enrichment results to identify the important biochemical metabolic pathways and signal transduction pathways involving the DEGs through matching to the KEGG database. The top 20 KEGG enrichment pathways were associated with metabolism, cellular processes, organismal systems and human diseases (Fig. 4). Only one statistically significant KEGG term (KEGG ID: ko04142) was detected and enriched in the lysosome pathway that were associated with 21 DEGs including GI IDs 119373383, 119373807, 119376241, 119381061, 119382561, 119382563, 119384031, 119386015, 119386803, 119389752, 119390141, 119391070, 119393341, 119396876, 119398877, 119399464, 119401661, 119404474, 119405483, 119406376 and MSTRG.26827. The two statistically significant GO terms mapped to 18 transcripts and the statistically significant KEGG term mapped to 30 transcripts (Table 1). During the blood meals of *R. sanguineus*, the unfed ticks sucked blood and became semiengorged ticks, a transition was associated with 31 upregulated and 9 downregulated transcripts.

Table 1. Key transcripts in regulating blood meals of *R. sanguineus* via Go and KEGG enrichment.

Accession No.	Descriptions	Levels	Enrichment analysis
XM_037643022	Phospholipase B-like 2	Up	GO
XM_037643405	Uncharacterized LOC119373383	Up	KEGG
XM_037643861	Uncharacterized LOC119373807	Up	KEGG
XM_037646144	NPC1-like intracellular cholesterol transporter 1	Up	KEGG
XM_037647522	Gamma-interferon-inducible lysosomal thiol reductase	Up	GO
XM_037650313	Alpha-galactosidase A	Down	KEGG
XM_037650315	Uncharacterized LOC119390141	Up	KEGG
XM_037652321	Sialin	Down	GO
XM_037652322	Sialin	Down	GO
XM_037654077	Uncharacterized LOC119386015	Up	GO/KEGG
XM_037657131	Legumain-like	Up	GO/KEGG
XM_037657701	NPC intracellular cholesterol transporter 2	Up	KEGG
XM_037658646	Beta-hexosaminidase subunit alpha	Down	GO
XM_037658650	Solute carrier family 35 member F6-like	Up	GO
XM_037658754	Solute carrier family 35 member F6	Up	GO/KEGG
XM_037660314	Arylsulfatase B	Up	KEGG
XM_037661722	Cubilin	Up	GO
XM_037664231	Cathepsin D	Up	GO/KEGG
XM_037665694	NPC intracellular cholesterol transporter 2	Up	KEGG
XM_037666262	Alpha-galactosidase A	Up	KEGG
XM_037666264	NPC1-like intracellular cholesterol transporter 1	Up	KEGG
XM_037666519	Sialomucin core protein 24	Up	GO
XM_037668578	Uncharacterized LOC119390141	Down	KEGG
XM_037670977	NPC intracellular cholesterol transporter 2	Up	KEGG
XM_037670978	Gastric triacylglycerol lipase	Up	KEGG
XM_037670979	Arylsulfatase B	Up	KEGG
XM_049412142	E3 ubiquitin-protein ligase MARCH2	Up	GO/KEGG
XM_049412239	Alpha-N-acetylgalactosaminidase	Down	KEGG
XM_049412741	Sialin	Down	GO/KEGG
XM_049414198	Lysosomal alpha-glucosidase	Up	GO/KEGG
XM_049417715	Uncharacterized LOC119373383	Up	KEGG
XM_049417716	Gastric triacylglycerol lipase	Up	KEGG
XM_049417717	Beta-galactosidase	Up	KEGG
XM_049417719	Alpha-N-acetylgalactosaminidase	Up	KEGG
XM_049417720	Uncharacterized LOC119373807	Up	KEGG
XM_049418654	Phospholipase B-like 2	Up	GO
XM_049418655	Phospholipase B-like 2	Up	GO
XM_049418893	NPC intracellular cholesterol transporter 2	Down	KEGG
XM_049419420	Alpha-N-acetylglucosaminidase	Up	GO/KEGG
XM_049420067	Beta-galactosidase	Down	KEGG

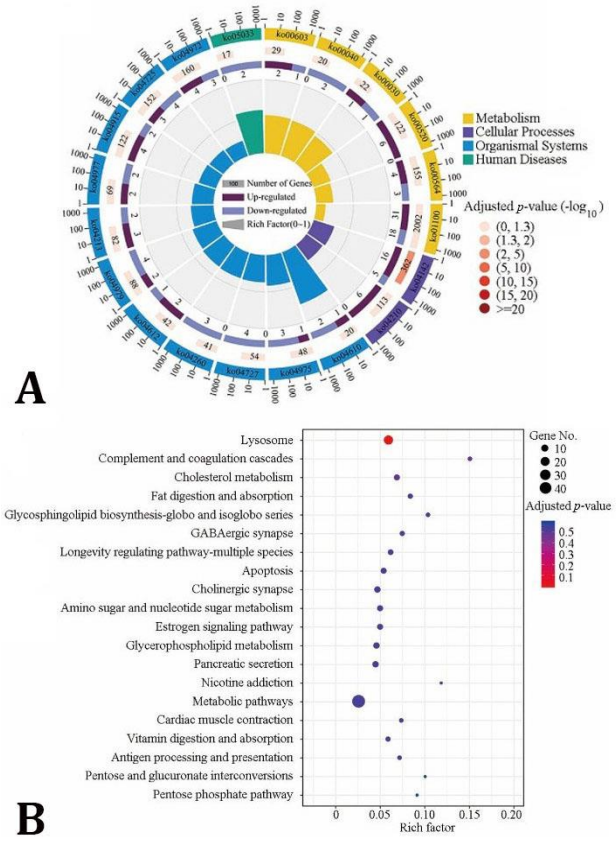

Fig. 4. Kyoto Encyclopedia of Genes and Genomes (KEGG) enrichment plot displaying the top 20 pathways listed in order of false discovery rate -adjusted *p* value from smallest to largest. **A)** The KEGG enrichment circle plot with 4 rings. From the outside to the inside, the first circle shows a coordinate scale for the number of Differentially expressed genes (DEGs) and the different colors of the first circle represent the 4 different KEGG classes, namely, metabolism (yellow bars), cellular processes (purple bars), organismal systems (blue bars) and human diseases (green bars). A longer bar indicates a larger number of enriched KEGG pathways and a redder color denotes a smaller adjusted *p* value in the second circle. The third circle illustrates the up- and downregulated expression ratios of DEGs with deep purple indicating the ratios of the upregulated genes, light purple representing the ratios of the downregulated genes and the respective ratios shown below. The innermost circle represents the enrichment factor values for each pathway with each grid line indicating 0.1. **B)** The KEGG enrichment bubble plot showing the top 20 pathways with the smallest adjusted *p* values. A larger bubble indicates a larger number of genes and a redder bubble denotes a smaller adjusted *p* value with the pathways shown on the Y-axis and the enrichment factors shown on the X-axis.

Discussion

Regarded as the most widespread three-host tick, *R. sanguineus* is of great importance in human and veterinary medicine causing an increasing and recurrent public health problem.[31] Blood-sucking, as a necessary behavior, inaugurates tick-pathogen-host interactions with large numbers of studies on this topic. It is well known that vertebrate blood is essential for the molting, development of tick larvae, nymphs, maturation, reproduction and egg laying of females. Consistent with the line "Everything you see exists together in a delicate balance" in the Walt Disney movie “The Lion King”, pathogen transmission occurs while ticks are interacting with human and animal hosts, and the three elements establish an inextricable relationship. Many specific genes were clearly demonstrated to be involved in the progression of blood meals and displayed up- or downregulation in response to blood meals before and after exogenous blood intake and the achievement of a complete blood meal elicited the termination of gene transcription and expression. Specific genes with dynamic changes during blood meals are discovered and substantiated via gene silencing using RNA interference (RNAi) technology such as the silencing of AamAV422 and AAS19 expression in *Amblyomma americanum* leading to significantly reduced blood meal size.[32,33] In an effort to identify and quantify many molecular markers, omics techniques, with rapid development, have been employed to explore bulk data, including DEGs and novel genes involved in various biological functions and intricate pathways.

In the present study, we utilized transcriptomic profiling to identify the key molecules involved in blood meal feeding in adult female *R. sanguineus*. Molecules with significantly different abundance levels have been the focus of attention in research exploring the physiological changes in response to a blood meal in comparisons of semiengorged and unfed female ticks. A total number of 744 transcripts consisting of 309 upregulated and 435 downregulated transcripts were significantly differentially expressed at the RNA level. Biological functional annotations of the target transcripts provided novel insight for choosing focal molecules in the process of blood meal intake. Out of the top 10 differentially upregulated transcripts, four were characterized as turripeptide OL55-like protein, valine tRNA ligase, ice-structuring glycoprotein-like protein and a predicted timeless-interacting protein, and six novel transcripts were unannotated sequences in accordance with the current reference transcript sequences available in the NCBI database. Nevertheless, out of the top 10 downregulated transcripts, two with GI accession numbers but not yet functionally described were clearly characterized, and the remaining eight novel transcripts did not match any sequences in the reference transcriptome datasets. Functional enrichment analysis revealed that the DEGs were associated with two GO terms with GO IDs 0000323 and 0005773 in the cellular component category: Lytic vacuole and vacuole. This was a novel and previously unreported finding. Pathway enrichment analysis revealed that 21 DEGs were involved in the KEGG lysosome pathway including 20 known genes and a novel gene

associated with intracellular digestion occurring in the tick MG epithelium.[34]

Considering that blood intake is the beginning of tick-host interactions our strategy was devised to explore in bulk the molecules exhibiting changes during vector-host interactions. The molecules in semiengorged showing significant differences from those in unfed ticks are of great interest in advancing our understanding of the mechanisms of blood meals. The present study provided differentially expressed transcripts that would be targeted for silencing by RNA interference technology in subsequent experiments to eventuate the ticks to fail to complete engorgement. In summary, key molecules annotated via transcriptomic approaches were anticipated to be nominees for intervening in tick-host interactions for the purpose of tick life termination and tick control.

Acknowledgments

The study was supported by grants from the Key Laboratory of Parasite Pathogen and Vector Biology of Healthy Ministry (No. NHCKFKT2021-10), the National Natural Science Foundation of China (82360028), and the Major Science and Technology Program of Hainan Province (No. ZDKJ2021036).

Conflict of interest

The authors declare no conflicts of interest.

References

1. Brophy M, Walker KR, Adamson JE, et al. Tropical and temperate lineages of *Rhipicephalus sanguineus s.l.* ticks (Acari: Ixodidae) host different strains of *Coxiella*-like endosymbionts. J Med Entomol 2022; 59(6): 2022-2029.
2. Garcia-Rosales L, Escarcega-Avila A, Ramirez-Lopez M, et al. Immune monitoring of paediatric patients infected with *Rickettsia rickettsii*, *Ehrlichia canis* and coinfected. Pathogens 2022; 11(11): 1351. doi: 10.3390/pathogens11111351.
3. Walker DH, Blanton LS, Laroche M, et al. A vaccine for canine Rocky Mountain spotted fever: an unmet one health need. Vaccines (Basel) 2022; 10(10): 1626. doi: 10.3390/vaccines10101626.
4. Namina A, Capligina V, Seleznova M, et al. Tick-borne pathogens in ticks collected from dogs, Latvia, 2011-2016. BMC Vet Res 2019; 15: 398. doi: 10.1186/s12917-019-2149-5.
5. Hazelrig CM, Gettings JR, Cleveland CA, et al. Spatial and risk factor analyses of vector-borne pathogens among shelter dogs in the Eastern United States. Parasit Vectors 2023; 16(1): 197. doi: 10.1186/s13071-023-05813-1.
6. Phiri BSJ, Kattner S, Chitimia-Dobler L, et al. *Rickettsia* spp. in ticks of South Luangwa Valley, Eastern Province, Zambia. Microorganisms 2023; 11(1): 167. doi: 10.3390/microorganisms11010167.
7. Springer A, Glass A, Probst J, et al. Tick-borne zoonoses and commonly used diagnostic methods in human and veterinary medicine. Parasitol Res 2021; 120(12): 4075-4090.
8. Burgio F, Meyer L, Armstrong R. A comparative laboratory trial evaluating the immediate efficacy of fluralaner, afoxolaner, sarolaner and imidacloprid + permethrin against adult *Rhipicephalus sanguineus* (*sensu lato*) ticks attached to dogs. Parasit Vectors 2016; 9(1): 626. doi: 10.1186/s13071-016-1900-z.
9. Ebani VV, Mancianti F. Entomopathogenic fungi and bacteria in a veterinary perspective. Biology (Basel) 2021; 10(6): 479. doi: 10.3390/biology10060479.
10. Oskam CL, Gofton AW, Greay TL, et al. Molecular investigation into the presence of a *Coxiella* sp. in *Rhipicephalus sanguineus* ticks in Australia. Vet Microbiol 2017; 201: 141-145.
11. Guccione C, Colomba C, Tolomeo M, et al. *Rickettsiales* in Italy. Pathogens 2021; 10(2): 181. doi: 10.3390/pathogens10020181.
12. Cardenas-Cadena SA, Castañeda-Lopez ME, Mollinedo-Montaño FE, et al. Tick-borne pathogens screening using a multiplex real-time polymerase chain reaction-based method. Acta Parasitol 2023; 68(3): 705-710.
13. Kidd L, Hamilton H, Stine L, et al. Vector-borne disease and its relationship to hematologic abnormalities and microalbuminuria in retired racing and show-bred greyhounds. J Vet Intern Med 2022; 36(4): 1287-1294.
14. Oleaga A, Carnero-Morán A, Valero ML, et al. Proteomics informed by transcriptomics for a qualitative and quantitative analysis of the sialoproteome of adult *Ornithodoros moubata* ticks. Parasit Vectors 2021; 14: 396. doi: 10.1186/s13071-021-04892-2.
15. Stewart PE, Bloom ME. Sharing the ride: *Ixodes scapularis* symbionts and their interactions. Front Cell Infect Microbiol 2020; 10: 142. doi: 10.3389/fcimb.2020.00142.
16. Li Z, Macaluso KR, Foil LD, et al. Inward rectifier potassium (Kir) channels mediate salivary gland function and blood feeding in the lone star tick, *Amblyomma americanum*. PLoS Negl Trop Dis 2019; 13(2): e0007153. doi: 10.1371/journal.pntd.0007153.
17. Sharma A, Pooraiiouby R, Guzman B, et al. Dynamics of insulin signaling in the black-legged tick, *Ixodes scapularis*. Front Endocrinol (Lausanne) 2019; 10: 292. doi: 10.3389/fendo.2019.00292.
18. Budachetri K, Kumar D, Crispell G, et al. The tick endosymbiont *Candidatus Midichloria* mitochondrii and selenoproteins are essential for the growth of *Rickettsia parkeri* in the Gulf Coast tick vector.

Microbiome 2018; 6(1): 141. doi: 10.1186/s40168-018-0524-2.
19. Abbas MN, Chlastáková A, Jmel MA, et al. Serpins in tick physiology and tick-host interaction. Front Cell Infect Microbiol 2022; 12: 892770. doi: 10.3389/fcimb.2022.892770.
20. Gargili A, Estrada-Peña A, Spengler JR, et al. The role of ticks in the maintenance and transmission of Crimean-Congo hemorrhagic fever virus: a review of published field and laboratory studies. Antiviral Res 2017; 144: 93-119.
21. Hernandez EP, Kusakisako K, Talactac MR, et al. Characterization and expression analysis of a newly identified glutathione S-transferase of the hard tick *Haemaphysalis longicornis* during blood-feeding. Parasit Vectors 2018; 11(1): 91. doi: 10.1186/s13071-018-2667-1.22.
22. Umemiya-Shirafuji R, Mihara R, Fujisaki K, et al. Intracellular localization of vitellogenin receptor mRNA and protein during oogenesis of a parthenogenetic tick, *Haemaphysalis longicornis*. Parasit Vectors 2019; 12: 205. doi: 10.1186/s13071-019-3469-9.
23. Liu L, Yan F, Zhang L, et al. Protein profiling of hemolymph in *Haemaphysalis flava* ticks. Parasit Vectors 2022; 15: 179. doi: 10.1186/s13071-022-05287-7.
24. Perner J, Hatalova T, Cabello-Donayre M, et al. Haem-responsive gene transporter enables mobilization of host haem in ticks. Open Biol 2021; 11(9): 210048. doi: 10.1098/rsob.210048.
25. de la Fuente J, Villar M, Cabezas-Cruz A, et al. Tick-host-pathogen interactions: conflict and cooperation. PLoS Pathog 2016; 12(4): e1005488. doi: 10.1371/journal.ppat.1005488.
26. Chen S, Zhou Y, Chen Y, et al. fastp: an ultra-fast all-in-one FASTQ preprocessor. Bioinformatics 2018; 34(17): i884-i890.
27. Langmead B, Salzberg SL. Fast gapped-read alignment with Bowtie 2. Nat Methods 2012; 9(4): 357-359.
28. Kim D, Langmead B, Salzberg SL. HISAT: a fast spliced aligner with low memory requirements. Nat Methods 2015; 12(4): 357-360.
29. Pertea M, Pertea GM, Antonescu CM, et al. StringTie enables improved reconstruction of a transcriptome from RNA-seq reads. Nat Biotechnol 2015; 33(3): 290-295.
30. Love MI, Huber W, Anders S. Moderated estimation of fold change and dispersion for RNA-seq data with DESeq2. Genome Biol 2014; 15(12): 550. doi: 10.1186/s13059-014-0550-8.
31. Dantas-Torres F, Otranto D. *Rhipicephalus sanguineus* (brown dog tick). Trends Parasitol 2022; 38(11): 993-994.
32. Kim TK, Radulovic Z, Mulenga A. Target validation of highly conserved *Amblyomma americanum* tick saliva serine protease inhibitor 19. Ticks Tick Borne Dis 2016; 7(3): 405-414.
33. Mulenga A, Kim TK, Ibelli AMG. Deorphanization and target validation of cross-tick species conserved novel Amblyomma americanum tick saliva protein. Int J Parasitol 2013; 43(6): 439-451.
34. Xu Z, Lin Z, Wei N, et al. Immunomodulatory effects of Rhipicephalus haemaphysaloides serpin RHS2 on host immune responses. Parasit Vectors 2019; 12(1): 341. doi: 10.1186/s13071-019-3607-4.

1st International Congress of Veterinary Medicinal Plants and Traditional Medicine

Topics:

- Plant Products and Pharmacology
- Effects of Plant Products on Animal and Zoonotic Pathogens
- Plant Products and Food Science
- Traditional Veterinary Medicine
- Phytochemistry and Biotechnology in Medicinal Plants

October 21 & 22 2024

Urmia - Iran

https://1icvmp.urmia.ac.ir
https://1icvmp.com

ISC
Islamic World Science Citation Center
03240-97388